Applied Catalysis B: Environmental 181 (2016) 24–33

Contents lists available at ScienceDirect

Applied Catalysis B: Environmental

journal homepage: www.elsevier.com/locate/apcatb

Study on the catalytic oxidation of DMDS over Pt-Cu catalysts supported on Al_2O_3, $AlSi_{20}$ and SiO_2

Bouchra Darif[a,b], Satu Ojala[a], Laurence Pirault-Roy[c], Mohammed Bensitel[b], Rachid Brahmi[b,*], Riitta L. Keiski[a]

[a] Environmental and Chemical Engineering Research Group (ECE), Faculty of Technology, P.O. Box 4300, FI-90014, University of Oulu, Finland
[b] Laboratory of Catalysis and Corrosion of Materials (LCCM), Department of Chemistry, Faculty of Sciences of El Jadida, University of Chouaib Doukkali, BP.20, 24000 El Jadida, Morocco
[c] Institute of Chemistry of Poitiers, Materials and Natural Resources (IC2MP), CNRS-UMR 7285, University of Poitiers B27, Rue Michel Brunet, 86073 Poitiers Cedex 9, France

ARTICLE INFO

Article history:
Received 20 May 2015
Received in revised form 21 July 2015
Accepted 25 July 2015
Available online 29 July 2015

Keywords:
Sulfur containing volatile organic compounds
Dimethyldisulfide
Pt-Cu catalysts
Stability
Environmental catalysis

ABSTRACT

Due to their harmful effects, finding the optimal catalysts for Sulfur containing Volatile Organic Compounds (S-VOC) oxidation is an important environmental challenge. A series of Pt-Cu catalysts supported on alumina (Al_2O_3), silica (SiO_2) and silica doped alumina $(Al_2O_3)_{0.8}(SiO_2)_{0.2}$ were prepared and tested in the catalytic oxidation of dimethyldisulfide (DMDS). Characterization of the catalysts revealed that the performance of the catalyst is related to the interaction between Pt-Cu active phase and the supports. DMDS conversion on the Pt-Cu/Al_2O_3 catalyst was found to be close to that of the Pt-Cu/$(Al_2O_3)_{0.8}(SiO_2)_{0.2}$ catalyst. However, doping the Al_2O_3 substrate by SiO_2 led to a more selective and stable catalyst.

1. Introduction

The treatment of waste gas emissions containing volatile organic compounds (VOCs) has become more important during the past 20 years. Concerning the treatment of organic waste gases, the abatement of those emissions containing sulfur, such as CH_3SH, $(CH_3)_2S$ and $(CH_3)_2S_2$ is crucial, because sulfur containing volatile organic compounds (S-VOCs) have a well-known unpleasant odor and they irritate skin and eyes already at very low concentrations. Moreover, volatile sulfur compounds are prominent air pollutants, causing significant environmental problems [1]. Dimethyl disulfide (DMDS) is used in this study as a model molecule, since it is often present in industrial effluents and it is difficult to oxidize when compared with other sulfur-containing compounds present in the waste gas streams.

Based on the literature, there are not numerous studies dealing with rather high concentrations of S-VOCs. For instance, Cellier et al., studied the degradation of 250 ppm of methanethiol using manganese sulfate catalyst [2]. Certain other studies have been dealing with low concentrations of DMDS in the gas phase, such as 84 ppm [3], and the degradation of 10 ppm of DMDS using photo-catalysts [4]. Wang et al. [5] studied DMDS oxidation using $CuO–MoO_3/\gamma$-Al_2O_3 catalysts with different promoters. For the activity evaluation they used concentration of 450 ppm and for the durability study (20 h) they used 70 ppm of DMDS. In our study, somewhat higher concentrations are used, since in the case of the pulp mill emission abatement, the S-VOCs are present in remarkably higher concentrations than in the studies done earlier. This is setting an important challenge to the catalyst development.

In wide perspective, many reactions are carried out using silica-alumina supported catalysts such as isomerization, alkylation of aromatic molecules, oligomerization of olefins, cracking [6] and deep hydrodesulfurization of gas oil in which silica also favors the hydrodenitrogenation [7,8]. Generally, the amorphous SiO_2-Al_2O_3 support is used for hydrocracking catalysts due to its favorable acidity [9–10]. It has been reported in the literature [11–13], that the combination of these two oxides (Al_2O_3 and SiO_2) has amorphous nature and a wide set of Lewis acid sites that could be the reason for

* Corresponding author.
E-mail address: rachid.brahmi@univ-poitiers.fr (R. Brahmi).

http://dx.doi.org/10.1016/j.apcatb.2015.07.050
0926-3373/

its high acidity compared to separate pure silica and pure alumina. Besides this important property, it was found that the amorphous SiO_2-Al_2O_3 support increases the material's resistance against sulfur poisoning [14,15]. Moreover, the low isoelectric point (IEP, i.e. 2.5) of SiO_2 can be enhanced by addition of alumina that improves the interaction between support and active metals [16]. Due to the previous information, these materials were selected for the current study. Indeed, one of the objectives of this work was to study the effect of the supports on the activity, selectivity and durability of the catalysts in the oxidation of dimethyldisulfide (DMDS).

Platinum is often recognized as the best noble metal for oxidation reactions, due to its interesting catalytic activity and selectivity. However, the application of Pt based catalysts is not always interesting, because they are expensive and they may be deactivated by poisoning, especially in the presence of compounds containing chlorine and sulfur [17,18]. The most active metal oxides in the total oxidation are the semiconductors of type P. The conduction is being made from positive holes in this type of semiconductors; the electrons are highly mobile and offer easy oxygen adsorption on the surface in anionic form such as O^- [19]. Chromium oxides [20], cobalt, copper [21] nickel and manganese [22] are the most commonly used. Both copper (I) and (II) oxides are P-type semiconductors and they find their applications in VOC abatement [23], in the abatement of CO [24] and NOx [25]. They are also very potential in S-VOC abatement, since they have beneficial properties against sulfur-deactivation [26]. The addition of a noble metal could increase further the activity and especially the selectivity of these catalysts. For this research, we selected an array of samples that included the three oxide supports, namely, alumina, silica, and silica doped alumina due to before mentioned properties. As the active phase Pt and Cu were used. The activities and selectivities of these catalysts were evaluated in the complete oxidation of DMDS with rather high concentration of 550 ppm. Furthermore, several characterization techniques were used to understand the results of catalytic testing.

2. Experimental

2.1. Catalyst preparation

In this work, Al_2O_3, (later denoted as Al), $(Al_2O_3)_{0.8}(SiO_2)_{0.2}$ (denoted as $AlSi_{20}$), and SiO_2 (denoted as Si), were used as support materials of the catalysts. The sol-gel preparation procedure used in this case involves three steps: preparation of a boehmite gel, drying and calcination.

The boehmite gel was synthesized with a method modified from the procedure described by Yoldas [27]. For this preparation, a known mass of aluminum tri-sec-butoxide ($Al[OCH(CH_3)CH_2CH_3]$, 97 %, Alfa Aesar) was mixed with ultrapure water corresponding to the molar ratio $n(H_2O)/n(Al) = 100$. The mixture was homogenized under stirring at 60 °C for 1 h. Then, two drops of hydrochloric acid (HCl) were added to catalyze the peptization reaction. The acid was introduced together with tetraethoxysilane ($Si(OC_2H_5)_4$, 99 %, Aldrich), which was the precursor of the dopant. Then the temperature was raised to 80 °C and kept constant for 2 h. During the synthesis, the reaction mixture was stirred and the beaker was covered with a watch-glass to minimize evaporation of water. Under these synthesis conditions (excess water, acid and temperature of 80 °C), the hydrated boehmite doped silica ($AlO(OH)$-$SiO_2 \cdot nH_2O$) was obtained.

The whitish gel obtained, was dried at 120 °C overnight, and then grounded, leading to the formation of a white powder of boehmite-type doped xerogel. After that, the powder was calcined at 550 °C for 5 h with a temperature rise of 5 °C min^{-1}.

The SiO_2 sol was prepared by hydrolysis and condensation reactions of tetraethoxysilane in the presence of nitric acid (HNO_3, Aldrich). The amounts of the reactants used in the preparation (in mol L^{-1}) are as follows: n(TEOS)/n(ETOH)/n(H_2O)/n(HNO_3) equals to 1/8/6/0.3. In the next preparation step, the mixture was stirred for 3 h and dried at room temperature for about three months, then calcined at 550 °C with a temperature rise of 5 °C min^{-1}.

The bimetallic Pt-Cu catalysts supported separately on the materials mentioned above with 0.3 wt% platinum, and 10 wt% copper loading, were prepared by the wet co-impregnation method using chloroplatinic acid hexahydrate ($H_2PtCl_6 \cdot 6H_2O$, 99.9%, Alfa Aesar) and copper(II) nitrate hemipentahydrate ($Cu(NO_3)_2 \cdot 2.5H_2O$, 98%, Alfa Aesar) as active phase precursors. After dissolving the precursors with ultrapure water and introducing the support material, stirring was continued at room temperature overnight. Then the sample was dried at 65 °C using a sand-bath. Finally, the catalyst samples 0.3Pt10Cu/Al, 0.3Pt10Cu/$AlSi_{20}$ and 0.3Pt10Cu/Si were calcined in air at 550 °C for 5 h.

2.2. Catalyst characterization

The final loading of platinum and copper on the catalysts was analyzed, after microwave-assisted sample digestion, using an inductively coupled plasma optical emission spectrometer (ICP-OES) (PerkinElmer Optima 5300 DV). The supports and catalysts were characterized by physisorption of N_2 at −196 °C performed on an automated volumetric apparatus Micrometrics ASAP2020 to find out the specific surface areas and the porosities. Identification of phases and crystallite size estimation were done by XRD measurement. The XRD data were collected at room temperature, using a Siemens D5000 diffractometer equipped with a Cu anode ($\lambda_{Cu} = 1.5418$ Å) and a nickel filter. Additional acquisition parameters were: 2θ range 5–90 °; step 0.025 ° and dwell time of 1 s. Diffraction patterns were compared to ICDD database (International Center for Diffraction Data) for identification of crystalline phases. The crystallite size of the active phase and support was estimated using the Scherrer formula:

$$D = \frac{k\lambda}{\beta_c \times \cos\theta} \quad (1)$$

where k is the shape factor ($k = 0.94$) and λ is the wavelength of X-ray;. θ is the Bragg angle and βc is the corrected line broadening defined as FWHM (full width at half maximum).

To obtain quantitative measures of particle and/or grain size, particle size distribution, and morphology, transmission electron microscopy (TEM) was performed by using a JEM-2100 LaB_6 equipped with an energy dispersive spectrometer EDS.

The reducibility properties were examined by temperature programmed reduction (TPR) carried out for calcined catalyst samples. In the experiment, after stabilization at 30 °C, the furnace temperature was increased to 500 °C with a rate of 5 °C min^{-1} and pulsed injections of hydrogen were sent to the reactor every 25 s using a constant flow rate of 30 cm^3 min^{-1} of 1% H_2 in Ar. The mass of the catalyst sample was 50 mg. The reduction was maintained for one hour at the final temperature. A magnesium perchlorate water trap was used to remove water from the outlet gas stream. The hydrogen consumption was monitored by a thermal conductivity detector (TCD).

The X-ray photoelectron spectroscopy (XPS) analyses of 0.3Pt10Cu/Si, 0.3Pt10Cu/Al and 0.3Pt10Cu/$AlSi_{20}$ were performed with a Thermo Fisher Scientific ESCALAB 250Xi X-ray photoelectron spectroscopy (XPS) system equipped with Al Kα X-ray source = 1486.7 eV to study the chemical states of copper and platinum elements. The X-ray source operated at 10 mA and 12 kV. The spectral regions corresponding to Cu 2p, Pt 4d, Pt4f, Al 2p and O 1s core levels were recorded for each sample. The static charge of the samples was corrected by referencing all binding energies (BE) to

the Al 2p peak (BE = 72.6 eV) except for the catalyst 0.3Pt10Cu/Si, the charging effects were corrected using the C1s peak (285 eV).

2.3. Catalyst testing

The activities of the catalysts were tested in the oxidation of (dimethyldisulfide DMDS) with the concentration of 550 ppm in 1 L min^{-1} of purified air at the temperature range from room temperature to 600 °C with 5 °C min^{-1} heating rate and gas hourly space velocity (GHSV) of 76,500 h^{-1}. The catalyst samples of 100 mg were put between two layers of 100 mg of quartz sand and then packed into a tubular reactor with quartz wool plugs. The gas composition was measured with an FTIR (Gasmet, Model Cr2000). The compounds followed by FTIR were dimethyl disulphide ($C_2H_6S_2$), methyl mercaptan (CH_4S), sulfur dioxide (SO_2), sulfur trioxide (SO_3), dimethyl sulphide (C_2H_6S), ethyl mercaptan (C_2H_6S), formaldehyde (CHOH), carbon monoxide (CO), carbon dioxide (CO_2), methane (CH_4), methanol (CH_4O) and water (H_2O).

The conversion of DMDS, and yields of the main products are defined in the following way:

$$\text{Conversion}(\%) = \frac{Ci - Co}{Ci} \times 100 \quad (3)$$

$$\text{Co}_2\ \text{Yield}(\%) = \frac{[CO_2]}{2xCi} \times 100 \quad (4)$$

$$\text{CO Yield}(\%) = \frac{[CO]}{2xCi} \times 100 \quad (5)$$

$$\text{and } SO_2\text{Yield}(\%) = \frac{[SO_2]}{2xCi} \times 100 \quad (6)$$

where C_i is the initial feed concentration of dimethyldisulfide DMDS (ppm), C_0 is the outlet concentration of DMDS (ppm), [CO_2], [CO] and [SO_2] are the concentrations of the corresponding compounds in mol L^{-1}.

3. Results and discussion

3.1. Characterization results

Fig. 1 shows the X-ray diffractograms of the prepared supports. Both, Al_2O_3 and $AlSi_{20}$ materials are semi amorphous while SiO_2 exhibits only an amorphous phase. In addition, the XRD data showed two different peaks at 46.48° and at 67.95° (according to ICDD standard 75-0921), which are the characteristic peaks for the γ-$A1_2O_3$ phase [28]. The XRD results evidenced the same structural properties for Al_2O_3, and doped alumina support $AlSi_{20}$ at 500 °C.

Fig. 2 shows the three diffraction patterns of the prepared catalysts. After the addition of platinum and copper, the diffraction data indicate the presence of γ-alumina for the catalysts that are supported on Al and $AlSi_{20}$, as expected from the previous results. These materials are, however, also mainly amorphous. Based on the literature available [9–15], the amorphus structure of the materials is potentially beneficial in our case.

The co-impregnation of the prepared $AlSi_{20}$ support by 0.3% of Pt and 10% of copper, did not change its amorphous phase. The peaks located at $2\theta = 35.05°$ and 38.18° that are assigned to the CuO crystalline phase [29] according to the ICDD database (01-089-2530) appeared in the diffractograms of 0.3Pt10Cu/Al and 0.3Pt10Cu/Si, but not for 0.3Pt10Cu/ $AlSi_{20}$.

Table 1 gathers together some physico-chemical properties of the prepared supports and catalysts. After the addition of 20% of silica, specific surface area of the support increased, which matched with the slight decrease in the crystallite size of the doped support. The crystallite size of the prepared catalysts and supports can be estimated using the XRD data by the Scherrer equation. Table 1 presents also the correlation between experimental and targeted loading of elements (i.e., platinum: 0.3 wt%, copper: 10 wt% and silica: 20 wt%) in the prepared catalysts.

The actual loading of supported metals remains relatively close to the targeted ones, thus, the support impregnation was successful. After the impregnation of the three different supports Al, $AlSi_{20}$ and Si, the specific surface area decreased in all cases (Table 1). Smallest decrease of S_{BET} in the case of 0.3Pt10Cu/Al was observed. This material maintained its amorphous phase in addition to 6 nm CuO crystallites formed. In the case of 0.3Pt10Cu/$AlSi_{20}$, the surface area decreased remarkably, which may indicate that the active phase is not as well-dispersed as on alumina support. However, CuO and Pt were not observed in the material and the crystallite sizes could not be determined by XRD. The most pronounced decrease of S_{BET} was observed for 0.3Pt10Cu/Si catalyst indicating that pore accessibility may be influenced due to the increase of CuO crystallite size (11 nm). The pore volume of calcined silica was 0.26 $cm^3\ g^{-1}$ and for

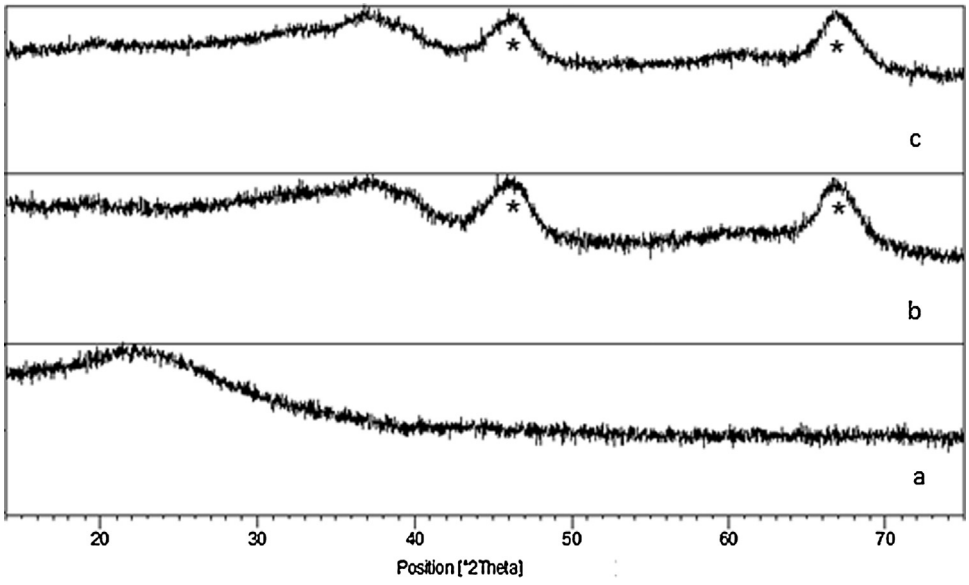

Fig. 1. XRD patterns for calcined prepared supports, (a) Si (b) $AlSi_{20}$ and (c) Al. (*) γ-alumina.

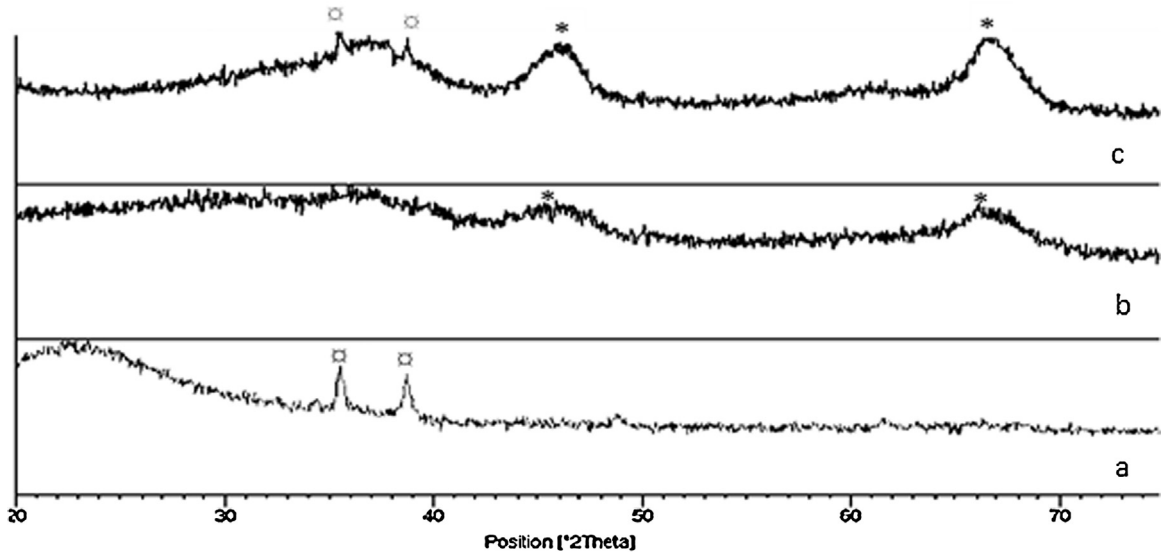

Fig. 2. XRD patterns for the prepared catalysts (a) 0.3Pt10Cu/Si, (b) 0.3Pt10Cu/$AlSi_{20}$, (c) 0.3Pt10Cu/Al, (*) Al_2O_3 and (¤) CuO.

Table 1
Physico-chemical properties of the prepared supports and catalysts.

Samples	Surface area (BET)/$m^2\ g^{-1}$	Crystallite size (XRD)/nm	Identified phase (XRD)	ICP/wt%		SiO_2
				Pt	Cu	
Al_2O_3	290	2.2	γ-Al_2O_3 and amorphous phase	–	–	–
$AlSi_{20}$	400	2	γ-Al_2O_3 and amorphous phase	–	–	16
SiO_2	540	nd	Amorphous phase	–	–	–
0.3Pt10Cu/Al	210	6 for CuO	Amorphous phase + CuO crystalline phase	0.3	9	–
0.3Pt10Cu/Al Si_{20}	150	2 for γ-Al_2O_3	γ-Al_2O_3	0.3	9	16
0.3Pt10Cu/Si	55	11 for CuO	amorphous phase + CuO crystalline phase	0.3	8	–

impregnated silica 0.03 $cm^3\ g^{-1}$ showing also the decrease in porosity.

In order to have more specific information about the morphology and composition of the prepared samples, TEM measurements were performed. Fig. 3 shows the TEM measurement results of (a) 0.3Pt10Cu/Al, (b) 0.3Pt10Cu/$AlSi_{20}$ and (c) 0.3Pt10Cu/Si. According to TEM coupled with EDX analysis, Pt was detected only on the copper particles in the case of 0.3Pt10Cu/Al and 0.3Pt10Cu/Si. It was not seen to exist alone on the surface, which indicates a close interaction between Pt and Cu species. Furthermore, in the case of 0.3Pt10Cu/Si catalyst, the bimetallic particles were larger than those on the other catalyst samples, which is in accordance with the drastic decrease in the specific surface area between the SiO_2 support and the corresponding impregnated sample (from 540 to 55 $m^2\ g^{-1}$) (Table 1).

For the 0.3Pt10Cu/$AlSi_{20}$ catalyst, the TEM images showed that copper exists as nanosized particles of somewhat more than 5 nm dispersed on the $AlSi_{20}$ support. In this sample, Pt particles were not visible at all with TEM.

The TPR experiments were performed to probe the reducibility of the bimetallic Pt-Cu catalysts. The H_2 consumptions after TPR measurement for the prepared catalysts were estimated assuming PtO and CuO formation during the calcination. This hypothesis is confirmed by the XPS results presented in the next section. The TPR results in Fig. 4 indicate that the reduction of the 0.3Pt10Cu/Si catalyst starts at about 127 °C, which is supported by the previous finding of Kazachkin et al. [30]. The TPR profile of the 0.3Pt10Cu/Si catalyst shows only one broad reduction peak at about 190 °C. This peak can be assigned to the reduction of Cu oxides. It is known that the reduction of Cu oxides is promoted by the presence of the noble

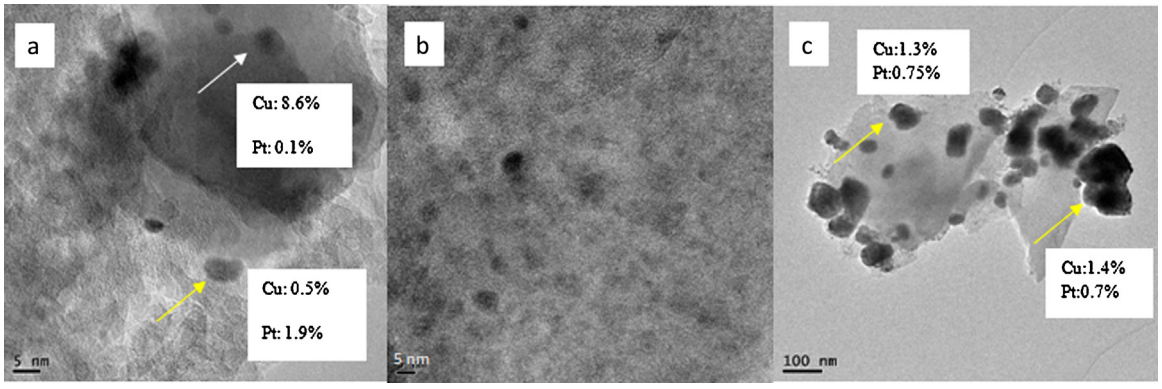

Fig. 3. TEM image of the catalysts (a) 0.3Pt10Cu/Al, (b) 0.3Pt10Cu/$AlSi_{20}$ and (c) 0.3Pt10Cu/Si.

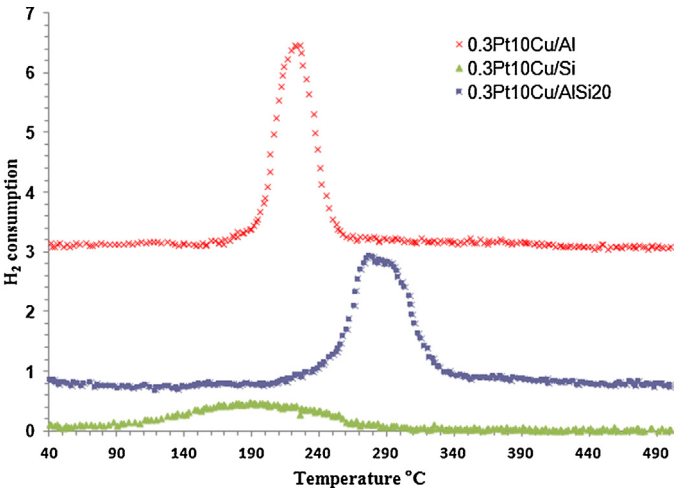

Fig. 4. TPR profiles for 0.3Pt10Cu/Al, 0.3Pt10Cu/$AlSi_{20}$ and 0.3Pt10Cu/Si catalysts.

metal [31,32], which is also visible in our case. This phenomenon indicates also that Cu and Pt species are in a close proximity, as observed by TEM. The enhancement of the reducibility is explained by the presence of platinum, which is needed to provide an abundant source of dissociated hydrogen, which due to spilling over from the Pt sites, contributes to the reduction of the copper oxide species. Moreover, these oxide species were expected to reduce rapidly, for another reason, because it has been reported that silica favors the hydrogen spillover as well, due to its enhanced hydrogen storage capacity after H_2 dissociation on the metallic surface [33]. Therefore, there would not be a deficiency of dissociated hydrogen in the proximity of copper particles even if Pt clusters, the source of dissociated H, would be quite distant [30].

The 0.3Pt10Cu/Al and 0.3Pt10Cu/$AlSi_{20}$ catalysts exhibited both a maximum temperature (T_{max}) in the range of 220–280 °C for the reduction of copper. These peaks can be observed at lower temperature than those generally observed for monometallic copper catalysts, which may indicate that the reduction of Cu oxides are also in these cases promoted by the presence of the noble metal. The differences in the reduction profiles are clearly indicative for the different supports used. The 0.3Pt10Cu/Al catalyst was reduced at lower temperature (220 °C) compared to the 0.3Pt10Cu/$AlSi_{20}$ catalysts (280 °C). In addition, the hydrogen consumption at 280 °C could be ascribed to the reduction of oxidized copper species not interacting with platinum, which is confirmed by TEM-EDX analysis [34]. Another explanation is that the lower reduction temperature of catalyst supported on alumina could be related to the crystalline CuO [35] and the higher one for the alumina-silica supported catalyst could be related to the reduction of amorphous CuO on γ-Al_2O_3 support, which phases are indicated by the XRD results.

Regarding to H_2 consumption calculations, a value of 0.5 was found for the 0.3Pt10Cu/Si, which is less than the expected value (1), meaning that the active phase is either still partly in the oxide form, exists already at the beginning of TPR in reduced form as a solid solution of Pt-Cu for example, or part of the metal is not accessible for reduction. Similarly, in the case of 0.3Pt10Cu/Al catalyst, the H_2 consumption calculation for bimetallic species gave a value of 0.87 that is lower than the expected value (1). After the addition of silica into alumina, the Pt and Cu oxide species were reduced completely assuming that copper existed as Cu (II). To summarize the results on reducibility, it can be concluded that the reduction of all samples is as complete as possible at 350 °C.

As it was discussed earlier, the studied catalysts showed different reduction temperatures, and according to TEM results, the 0.3Pt10Cu/$AlSi_{20}$ and 0.3Pt10Cu/Al catalyst exhibit rather small copper particle size. Sales et al., reported that supported CuO reduction temperature depends on the particle size and its interaction with the support [36]. Another study made by Epron et al. explained that it could be assumed that oxidized copper particles in the bimetallic catalyst are well-dispersed and interact strongly with the support, which is the most probable explanation for their higher reduction temperature [34]. From TPR results, it can be evaluated that the size of the copper particles is bigger on 0.3Pt10Cu/Si (exhibits lower reduction temperature) than on 0.3Pt10Cu/Al and 0.3Pt10Cu/$AlSi_{20}$. This evaluation is perfectly in accordance with the TEM results.

Table 2
Fresh and used catalysts characterization by XPS.

Samples	Pt $4f_{7/2}$ (eV)	Pt 4d (eV)	Cu $2p_{3/2}$ (eV) CuO	Pt species
0.3Pt10Cu/Si fresh	74.1		933.7	PtO_2
0.3Pt10Cu/$AlSi_{20}$ fresh		317.2	933.68	PtO
0.3Pt10Cu/$AlSi_{20}$ used		315	934	Pt (0)
		318.5		PtO_x
0.3Pt10Cu/Al fresh		315.2	933.8	Pt (0)
		318.9		PtO_2
		312.6		Pt-Cu
0.3Pt10Cu/Al used		312.7		Pt-Cu
		318		PtO_2

X-ray photoelectron spectra of the different Pt-Cu catalysts were measured with the aim of identifying the oxidation state of copper and platinum species. First, there is a known problem related to the XPS study in the case of Pt/Al_2O_3 catalysts, because the Al 2p line of the Al_2O_3 support overlaps with the Pt 4f line of the active phase usually used for the spectroscopic analysis of platinum. This makes the direct analysis of the platinum states very complicated and for that reason, a different line, Pt 4d, has been used in this study, which is not overlapping with the other spectral lines.

The decomposition of the spectra to individual components of Pt $4d_{5/2}$ core-level (Table 2) showed the presence of three different platinum species in the case of fresh 0.3Pt10Cu/Al catalyst (Fig. 5a). The peak component with BE (Pt$4d_{5/2}$) around 315.2 eV is assigned to the Pt (0) state and the last one located at 318.9 eV originates from the oxidized platinum species PtO_2. The third peak centered at 312.6 eV corresponds to Pt (0) belonging to the Pt-Cu alloy or to the intermetallic compound [37], which finding confirmed the presence of particles containing both Pt and Cu found by TEM-EDS measurements.

The sample used in DMDS oxidation showed a Pt 4d5/2 peak, which could be resolved after curve fitting procedures into two components with binding energies of 312.7 eV assigned to Pt (0) belonging to the Pt-Cu alloy or to the intermetallic compound [37] and another with a binding energy of 318 eV (Fig. 5-b). This component can be ascribed as PtO_x or likely as PtO_2 species [38]. Table 2 shows also that a part of Pt exists as metallic platinum in the fresh catalyst, which can explain the less than expected consumption of H_2 during TPR measurement of 0.3Pt10Cu/Al catalyst.

The binding energy of the Pt$4d_{5/2}$ at about 317.2 eV for 0.3Pt10Cu/$AlSi_{20}$ fresh (Fig. 6a) indicates that Pt is present in oxidized form (PtO) [39]. After the catalytic test in DMDS oxidation (Fig. 6b), the binding energies of the Pt$4d_{5/2}$ revealed two components with binding energies of around 315 eV, which is assigned to Pt (0) and around 318.5 eV that shows that Pt is present also in PtO_x form. This assignment of the Pt oxidation state is difficult, and data in the literature is rather contradictory complicating the interpretation of the results. For the catalyst 0.3Pt10Cu/Si (Fig. 10), the decomposition of the spectra to individual components of Pt 4f core-level revealed the presence of oxidized platinum (PtO_x) species in the bimetallic catalysts. The peak components with BE (Pt $4f_{7/2}$) and (Pt $4f_{5/2}$) around of 74.1 and 77.4 eV, respectively, reveal

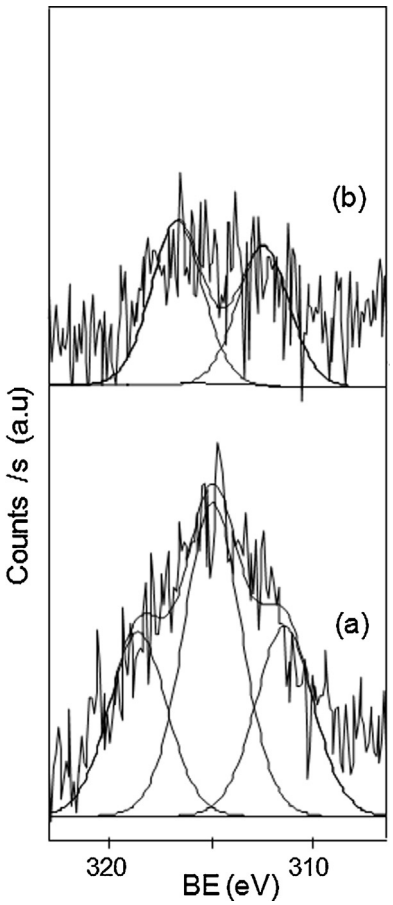

Fig. 5. Pt 4d5/2 core level spectra of 0.3Pt10Cu/Al. (a) Fresh, (b) after test.

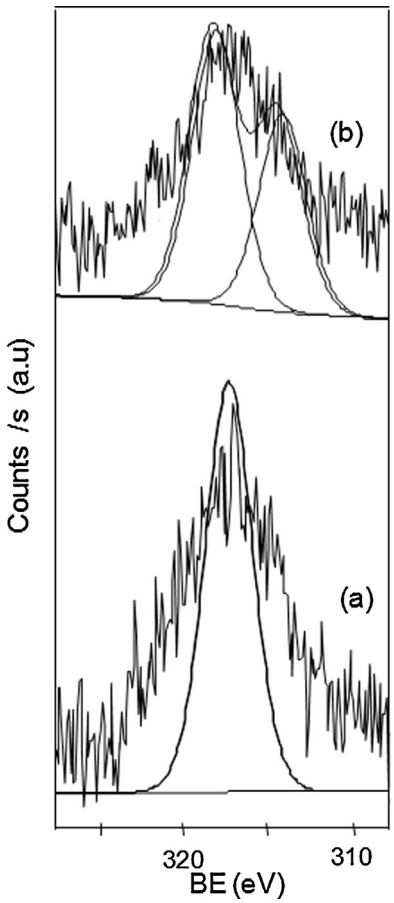

Fig. 6. Pt 4d5/2 core level spectra of 0.3Pt10Cu/$AlSi_{20}$. (a) Fresh, (b) after test.

that the Pt species on the surface of the catalyst exist as PtO_2 [40]. Concerning copper in all the fresh and used catalysts (Figs.7–9), the most intense peak (Cu $2p_{3/2}$) of the Cu 2p line at a binding energy around 933.68–933.8 eV and the appearance of the satellite-lines on each component of the Cu 2p are showing that copper is present as CuO on all the catalysts [41].

The homogeneous dispersion of copper on the Al and $AlSi_{20}$ surfaces observed for the corresponding catalysts is also validated by the close atomic ratios of Cu/Al (0.1) and Cu/$AlSi_{20}$ (0.083) obtained from XPS with respect to the predicted values Cu/Al (0.17) and Cu/$AlSi_{20}$ (0.15) derived from their nominal composition.

In the 0.3Pt10Cu/Si catalyst, the calculated XPS Cu/Si atomic ratio was higher (0.13) than the bulk value derived from its chemical composition (0.09) indicating the presence of an overlayer of copper species. The higher value of the surface Cu/Si ratio for the silica supported catalyst indicates the potential presence of aggregates of copper on the surface, which is in line with the TEM that showed the existence of large particles of copper species on the SiO_2 support. The XPS Pt/Si surface ratio for the same sample, summarized in Table 3, is higher than the calculated value derived from its chemical composition (Pt/Si = 0.007). This may be indicative for a platinum enrichment on the external surface of the support particles. However, since only a low metal loading was used, the possible covering of the silica support by Pt species can be ruled out. Another hypothesis could explain this dissimilarity between the XPS and theoretical Pt/Al ratios. According to TEM results, no Pt particles were seen to exist alone on the support SiO_2, but only on the large particles of Cu, and thus, Pt could be remote from Si species, which could be the reliable reason for this difference in the surface ratio of Pt/Si. In spite of this, the variations in the calculated XPS Pt/Al ratios

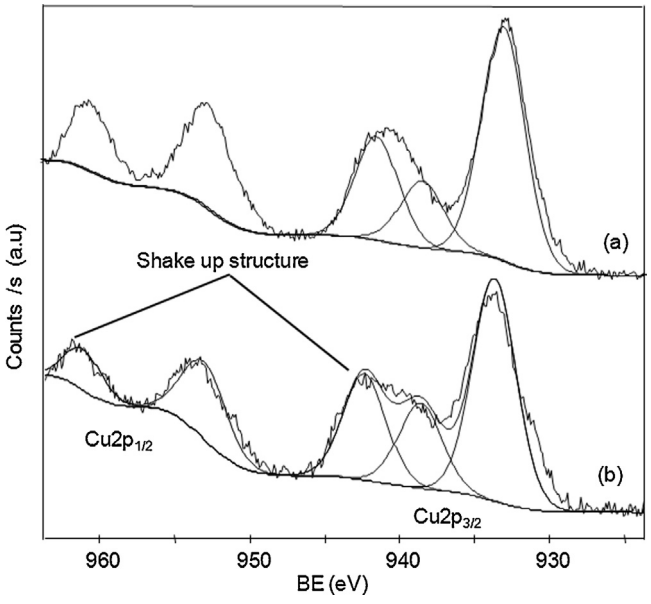

Fig. 7. Cu 2p3/2 spectra of 0.3Pt10Cu/Al. (a) Fresh, (b) after test.

indicate that there are changes occurred in the case of Pt surface concentration between fresh and used catalysts.

After DMDS oxidation, the surface dispersion of the active phase remarkably changed in the case of 0.3Pt10Cu/Al, according to XPS measurement (Table 3), the atomic ratio of Pt/Al (0.002) and Cu/Al (0.059) decreased indicating that the surface of the used catalyst

Table 3
Surface atomic ratios of fresh and used catalysts by XPS.

Sample	Pt/Si	Cu/Si	Pt/Al	Cu/Al	Si/Al	S/catalyst
0.3Pt10Cu/Si fresh	0.01	0.1				
0.3Pt10Cu/$AlSi_{20}$ fresh			0.004	0.083	0.165	
0.3Pt10Cu/Al fresh			0.0033	0.1		
0.3Pt10Cu/$AlSi_{20}$ used			0.0036	0.066	0.165	0.012
0.3Pt10Cu/Al used			0.002	0.059		0.029

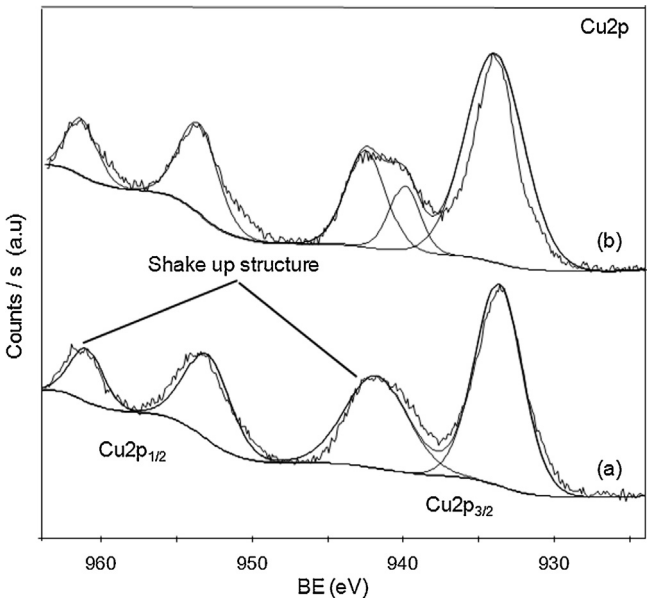

Fig. 8. Cu 2p3/2 spectra of 0.3Pt10Cu/$AlSi_{20}$. (a) Fresh, (b) after test.

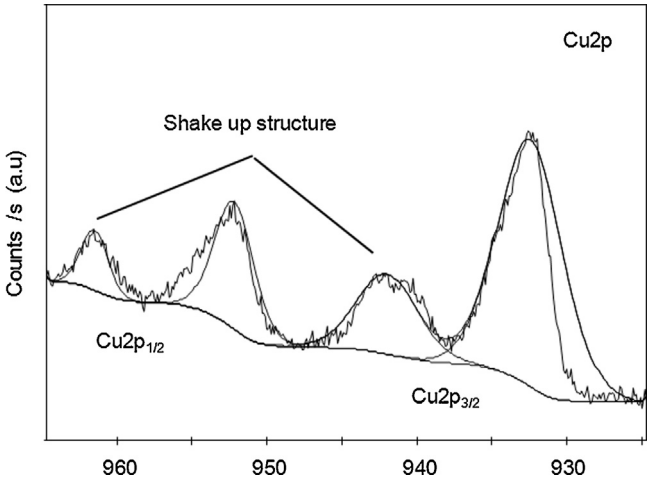

Fig. 9. Cu 2p3/2 spectra of 0.3Pt10Cu/Si fresh.

was exposed to certain chemical poisoning, most probably to sulfur species that were coming from the by-products or from DMDS compound itself. In the case of 0.3Pt10Cu/$AlSi_{20}$ the decrease in the dispersion of Pt (0.0036) and Cu (0.066) was detected as well, but it was not as severe as in the case of the 0.3Pt10Cu/Al catalyst. Besides, the elemental concentration of sulfur on the surface of 0.3Pt10Cu/Al was higher (0.029) than the one found in 0.3Pt10Cu/$AlSi_{20}$ (0.012). The surface concentration of Si on alumina oxide remained the same (0.165), which is supporting the finding that silica doping increases the resistance of alumina against sulfur.

According to Corro et al., the catalyst that is more sensitive to sulfation contains more highly oxidized Pt species on the

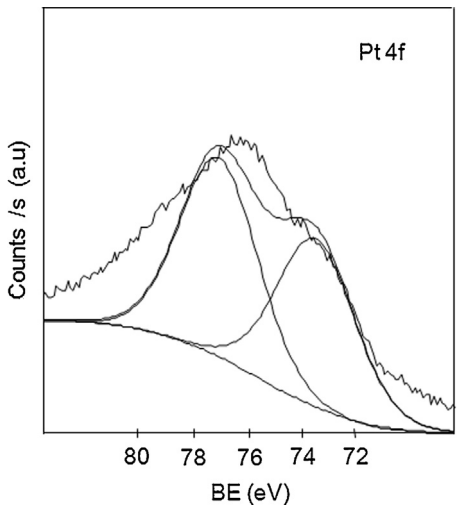

Fig. 10. Pt 4f core level spectra of 0.3Pt10Cu/Si fresh.

surface [39]. This is in accordance with our finding related to PtCu/Al catalyst, which exhibited presence of Pt^{4+} species in connection of higher concentration of sulfur on the surface in comparison to 0.3Pt10Cu/$AlSi_{20}$ catalyst that contained Pt^{+2} species.

3.2. Catalytic oxidation of dimethyldisulfide

The catalytic activity test results are shown in Fig. 11 for the three different catalyst samples. It can be observed in general, that the oxidation of DMDS is obviously influenced by the nature of the support of the catalysts. Moreover, the DMDS light-off curve indicates no significant competition between the catalytic and the thermal oxidation.

It can be seen from Fig. 11 that all the studied catalysts reached close to 100% conversion for DMDS, but 0.3Pt10Cu/Si catalyst was remarkably less active. In terms of catalytic activity, the light-off temperature of reaction was significantly lower than in the case of thermal experiment, but the reaction rate indicated by the tangent of the light-off curve was lower than in the case of the other two catalysts.

Over the catalyst supported on $AlSi_{20}$, about 100% DMDS conversion was reached at 440 °C. The reaction products detected were SO_2, CO_2 and H_2O with only slight formation of CO indicating good selectivity. The catalyst supported on Al showed slightly better activity in terms of lower oxidation temperature, other studies showed good results using CuO/γ-Al_2O_3 catalyst or the same promoted with Cr and Mo, the final catalysts were confirmed as active catalysts for the oxidation of DMDS with rather lower concentrations varied between (84 ppm and 450 ppm) [3,5]. Concerning the selectivity of our catalysts, significant formation of CO as an incomplete oxidation product was observed in addition to small amounts of certain organic intermediate products, such as, methanol (CH_2OH) and formaldehyde (CH_2O). All the catalysts showed high selectivity towards SO_2 formation.

The difference between the 0.3Pt10Cu/Al and 0.3Pt10Cu/$AlSi_{20}$ catalysts in the catalytic behavior can be explained by the

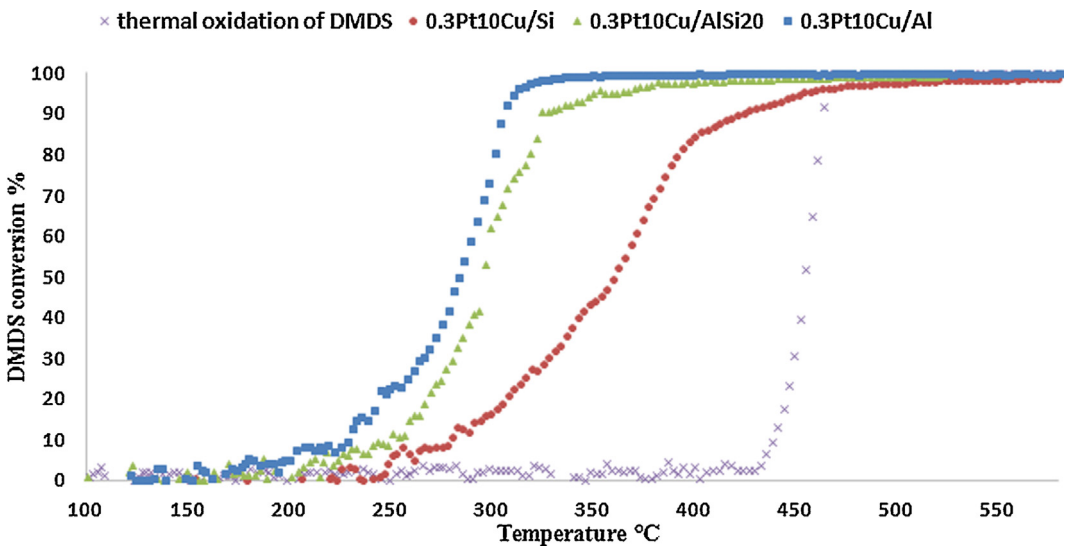

Fig. 11. Light-off curves of DMDS oxidation over 0.3Pt10Cu/ Al, 0.3Pt10Cu/ $AlSi_{20}$ and 0.3Pt10Cu/ Si. (DMDS 550 ppm, $m_{catalyst}$ = 100 mg, R_T −550 °C, 5 °C min^{-1}).

difference in the textural and structural properties of these catalysts. 0.3Pt10Cu/Al catalyst was highly active in terms of lower oxidation temperature, which advantage may be related to the existence of an alloy or intermetallic compound of Pt-Cu on the surface exhibiting well dispersed of 5 nm particles estimated by TEM-EDX Furthermore, the catalytic activity test with mechanical mixture between 0.3Pt/Al and 10Cu/Al showed that DMDS was completely oxidized, but at higher temperature range compared to the co-impregnated PtCu/Al catalyst. This finding proves that the interaction between Pt and Cu species is advantageous for the DMDS oxidation reaction in the case of 0.3Pt10Cu/Al catalyst. Moreover, the 0.3Pt10Cu/Al catalyst had higher specific surface area than the other prepared catalysts (Table 1). The close contact cannot be the only explanation for the higher activity, since the close contact of Pt and Cu species was also observed in the case of silica supported catalyst. However, in the case of 0.3Pt10Cu/Si, the particle size of the active phase is completely different. Thus, for good activity, the optimal nano-sized particles of around 5 nm dispersed on high surface area support are needed in addition to close contact between copper and platinum.

According to DMDS oxidation reaction (Eq. (7)), the catalytic oxidation of DMDS should finally lead to the formation of CO_2, SO_2 and H_2O.

$$CH_3 - S - S - CH_3 + \frac{11}{2}O_2 \rightarrow 2SO_2 + 2CO_2 + 3H_2O \quad (7)$$

Table 4, that represents the formed reaction by-products in mol L^{-1}, shows that the by-product content at the end of the catalytic reaction over 0.3Pt10Cu/$AlSi_{20}$ matched well with the theoretical values (Eq. (7)), and it can be observed that only traces of CO are formed. However, in the case of 0.3Pt10Cu/Al and 0.3Pt10Cu/Si, about 0.9 and 0.8 mol L^{-1} of CO are observed, respectively. The results show that 0.3Pt10Cu/$AlSi_{20}$ has almost similar activity than 0.3Pt10Cu/Al for DMDS oxidation, but the formation of CO_2 and SO_2 is closer to the targeted values.

The catalytic oxidation of S-VOCs does not require only high activity, but the ability to direct reaction to yield the desired reaction products is required as well. Especially, over-oxidation of sulfur to SO_3 leading to H_2SO_4 formation should be avoided and theoretic maximum of SO_2 formation should be aimed. In addition, due to the presence of sulfur, the stability of the catalyst plays an important role.

3.3. Stability of the catalysts in DMDS oxidation

Concerning stability, an improvement is expected by using the Al_2O_3-SiO_2 support, since it has been found that the amorphous Al_2O_3-SiO_2 phase increases the resistance of a supported catalyst against sulfur poisoning [14,15]. For that reason and based on the activity experiments, the most active catalyst 0.3Pt10Cu/Al and the most selective one 0.3Pt10Cu/$AlSi_{20}$ were chosen for a long-term stability test in DMDS oxidation at constant temperature of 400 °C. For the 0.3Pt10Cu/$AlSi_{20}$ catalyst, according to established results, no obvious decrease in the catalyst performance was observed during the 30 h test. The DMDS conversion stayed stable at about 99%. In the activity of 0.3Pt10Cu/Al, a decrease of 3% was observed already after 6 hours of time on stream. Moreover, there was no noticeable decline in the selectivity towards SO_2 during the stability test for both of the catalysts.

After 30 h of stability test, the light-off tests were carried out for the 0.3Pt10Cu/Al and 0.3Pt10Cu/$AlSi_{20}$ catalysts to compare the behavior of the fresh and used catalysts. According to the results shown in Fig. 12, the catalytic activity of the studied catalyst seems to be promoted after the ageing experiments in the temperature range of 150–290 °C, which may be due to the rearrangement of the catalyst active surface (will be studied in the future). At higher temperature range, it was observed that the DMDS conversion over 0.3Pt10Cu/$AlSi_{20}$ was slightly decreased as well as T_{90}, which was shifted from 320 °C for the fresh catalyst to 400 °C for the used one (see Table 5). T_{50} was shifted to lower temperature from 298 °C to 225 °C. Moreover the selectivity was observed to be stable towards

Table 4
Comparison of the catalytic reaction products at the outlet steam for 0.3Pt10Cu/Al, 0.3Pt10Cu/$AlSi_{20}$ and 0.3Pt10Cu/Si catalysts.

Prepared samples	0.310Pt10Cu/Al	0.3Pt10Cu/$AlSi_{20}$	0.3Pt10Cu/Si	Expected values
CO (mol L^{-1}) 10^{-5}	0.9	0.2	0.8	≈0
CO_2 (mol L^{-1}) 10^{-5}	2.8	2.4	1.6	2
SO_2 (mol L^{-1}) 10^{-5}	2.2	2.0	2.6	2

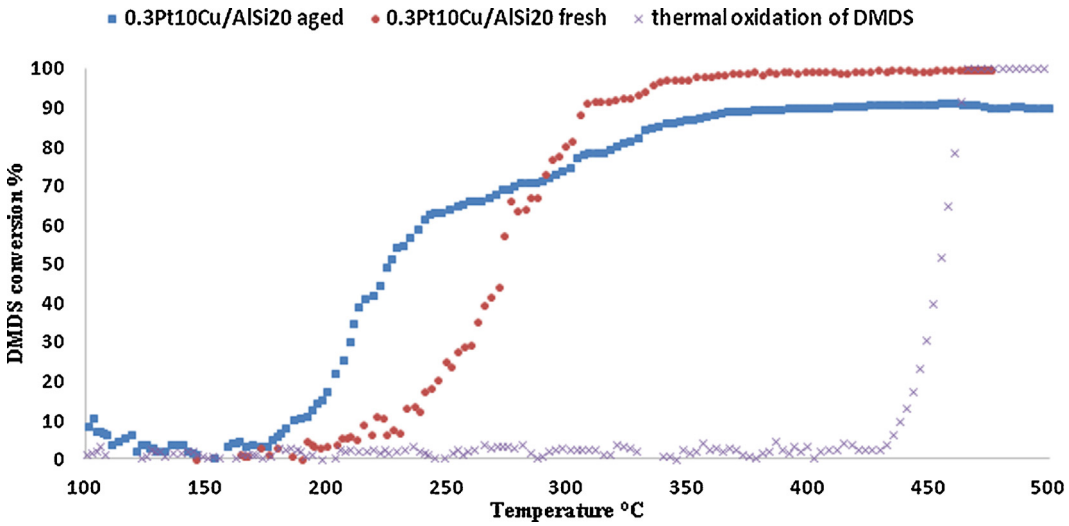

Fig. 12. Light off curves of DMDS oxidation over 0.3Pt10Cu/$AlSi_{20}$ before the ageing and after 30 h time on stream.

Table 5
T_{90} and T_{50} for DMDS oxidation over the fresh and used (after stability tests) catalysts.

Studied catalysts	0.3Pt 10Cu/ Al	0.3Pt 10Cu/$AlSi_{20}$	0.3Pt 10Cu/Si
T_{90} for fresh (°C)	310	320	480
T_{50} for fresh (°C)	285	298	362
T_{90} for used (°C)	≥500	400	–
T_{50} for used (°C)	330	225	–

Table 6
SO_2, CO_2 and CO yields for 0.3Pt10Cu/Al and 0.3Pt10Cu/$AlSi_{20}$ catalysts after stability tests.

Catalysts	0.3Pt10Cu/Al	0.3Pt10Cu/$AlSi_{20}$
SO_2 (%)	100	100
CO_2 (%)	69	98
CO (%)	21	6

SO_2 (100% yield) and CO_2 (98–99%) formation in addition to a slight formation of CO about 6% (See also Table 6). However, the carbon balance was observed to exceed 100%, which can be explained by the adsorption and the accumulation of DMDS on the catalyst surface in the beginning of the reaction. When temperature was increased, the catalyst started to release the accumulated DMDS at the same time with the recently adsorbed DMDS, which affected the carbon balance calculation.

Concerning the 0.3Pt10Cu/Al catalyst, the results in Fig. 13 show that the activity was changed and deteriorated drastically. The T_{50} value was shifted to higher temperature from 285 °C to 330 °C (see Table 5), as well as the T_{90} was shifted from 310 °C to over 500 °C. Besides, a decrease in the selectivity towards CO_2 was observed, a CO_2 yield of 69% was measured and 21% for CO formation (the SO_2, CO_2 and CO yields were measured at the end of the stability tests) (see Table 6). Furthermore, not only CO was observed during the catalytic oxidation experiment, but some other by-products were formed too, e.g. methanol (CH_4OH) and dimethysulfide (C_2SH_6). According to XPS analysis, alumina supported catalyst was vulnerable against the deactivation due to sulfur. Furthermore, there has been a noticeable accumulation of sulfur on the surface of alumina supported catalyst as well as decline in Pt and Cu surface dispersion on the support. However the $AlSi_{20}$ supported catalyst showed certain resistance against sulfur. XPS analysis indicated a low concentration of sulfur on the surface of the catalyst after the stability test as well as higher dispersion of Pt and Cu species com-

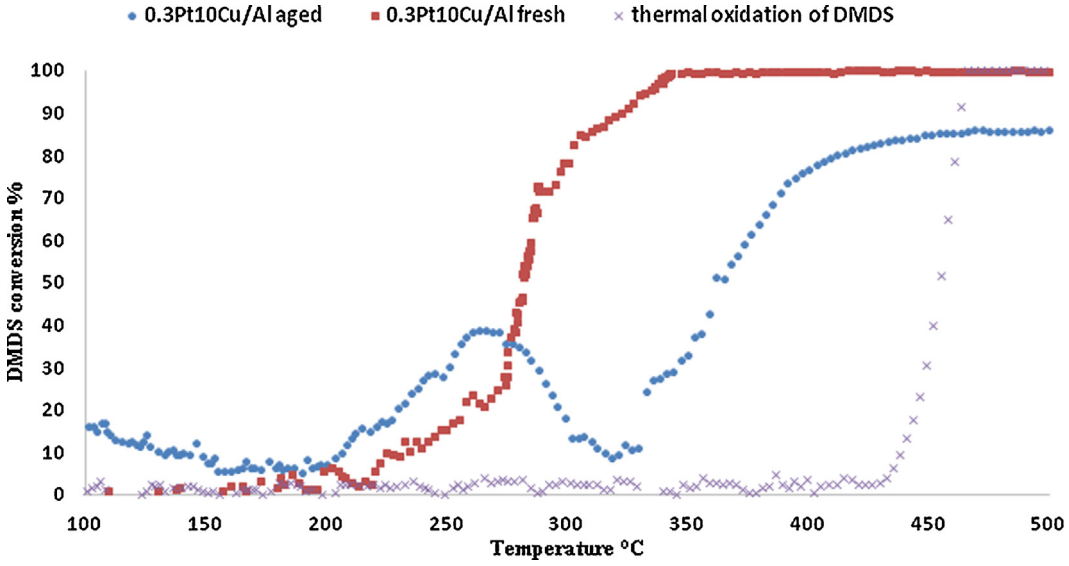

Fig. 13. Light off curves of DMDS oxidation over 0.3Pt10Cu/Al before the ageing and after 30 h time on stream.

pared to alumina supported catalyst. Thus, less than 20% of SiO_2 provided a potential resistance and tolerance to sulfur poisoning. Another explanation could be that the addition of SiO_2 onto γ-Al_2O_3 decreased the surface basicity and increased the surface acidity of the catalyst, providing a good condition to enhance desorption of SO_2 molecules from the surface of the catalyst after its formation during DMDS oxidation reaction. A number of different groups have investigated that strong SO_2 adsorption could occur at basic sites [42–44].

Dalla Lana et al. determined that the interaction of SO_2 with basic sites on the surface of γ-Al_2O_3 led to the formation of chemisorbed SO_2 [42]. Another study made by Karge et al., showed that strong chemisorption of SO_2 occurs on basic sites, whereas acidic sites seem to be responsible for weak adsorption [45]. Therefore, the effect of the surface acidity and basicity on the activity and selectivity of the catalyst is planned to be studied in more detail.

According to the results discussed previously and the data shown in Table 6, the selectivity of the prepared catalysts towards the desirable products CO_2 and SO_2, could be associated to the following parameters. The first is the easy reducibility character of the studied catalyst. It can be observed that the 0.3Pt10Cu/$AlSi_{20}$ catalyst that had a complete reduction of their oxide species of Pt and Cu, was found as the most selective one in DMDS oxidation. It showed 100%, 98% and only 6% of SO_2, CO_2 and CO yields respectively. Concerning the 0.3Pt10Cu/Al catalyst that showed an uncompleted reduction of the oxide species of Pt and Cu, only 69% as CO_2 yield and significant 21% yield of CO were observed. Furthermore, the second important parameter is that the chemical nature of the formed oxide phases of Pt on the surface seem to be central for the development of more efficient and selective Pt-Cu catalysts for the oxidation of DMDS. From the observed oxides of platinum, PtO seemed to create a good synergy with CuO on the $AlSi_{20}$ support material. Thirdly, most probably the acido-basic properties have an effect on the sulfur tolerance of the catalyst.

4. Conclusion

From the obtained results of the present study on the catalytic oxidation of DMDS, the following conclusions can be drawn:

1 Three different properties that affect the activity, selectivity and stability of the catalysts in DMDS oxidation are the texture, chemical structure, and the catalyst reducibility properties.
2 Among the three different types of Pt-Cu supported catalysts, the 0.3Pt10Cu/Al catalyst exhibits the highest activity for the DMDS oxidation based on the conversion. According to TPR, TEM and XPS results, there are close interaction between Pt and Cu (intermetallic Pt-Cu) in the nanosized scale, which could be one reason why this catalyst was highly active. The other reason can be the higher surface area of the 0.3Pt10Cu/Al catalyst shown by the BET values.
3 $AlSi_{20}$ was observed to be the most optimal support for Pt-Cu based catalysts in the oxidation of DMDS, since the 0.3Pt10Cu/$AlSi_{20}$ catalyst exhibits high activity, but also improved stability compared to the prepared 0.3Pt10Cu/Al catalyst. According to XPS results, it seems that the $AlSi_{20}$ support can resists sulfur poisoning better than alumina alone. 0.3Pt10Cu/$AlSi_{20}$ is also more selective than the other prepared catalysts.
4 The increased number of desorbed SO_2 molecules from the surface of the catalyst after its formation during DMDS oxidation reaction, could be linked to surface acidity of the support $AlSi_{20}$, which could be one reason to resist against sulfur poisoning. However, this issue should be studied in more detail.

Acknowledgments

The work was carried out with the financial support of the Council of Oulu Region from European Regional Development Fund via Sulka-project (A32164, 524/2012), the University of Oulu Graduate School (ADMA-DP/UniOGS) and PHC Volubilis Project (France-Morocco-Finland).

I would like to thank Ms. Kirsi Ahtinen (ECE, University of Oulu, Finland), Mr. Jorma Penttinen (ECE, University of Oulu, Finland), Jean-Dominique Comparot (IC2MP, Poitiers, France), and Stephane Pronier (IC2MP, Poitiers, France) for their help during the characterization of the catalysts.

The devices at the Center of Microscopy and Nanotechnology (CMNT) at the University of Oulu were used in the research.

References

[1] C.H. Wang, H.S. Weng, Ind. Eng. Chem. Res. 36 (1997) 2537–2542.
[2] C. Cellier, E.M. Gaigneaux, P. Grange, J. Catal. 222 (2004) 255–259.
[3] C.-H. Wang, H.-S. Weng, Ind. Eng. Chem. Res. 36 (1997) 2537–2542.
[4] Y.-H. Lin, T.-K. Tseng, H. Chu, Appl. Catal. A. 469 (2014) 221–228.
[5] C.-H. Wang, S.-S. Lin, S.-B. Liou, H.-S. Weng, Chemosphere 49 (2002) 389–394.
[6] M.F. Williams, B. Fonfeí, C. Sievers, A. Abraham, J.A. van Bokhoven, A. Jentys, J.A.R. van Veen, J.A. Lercher, J. Catal. 251 (2007) 485–496.
[7] N. Kunisada, K.H. Choi, Y. Korai, I. Mochida, K. Nakano, Appl. Catal. A Gen. 273 (2004) 287–294.
[8] N. Kunisada, K.H. Choi, Y. Korai, I. Mochida, K. Nakano, Appl. Catal. A Gen. 279 (2005) 235–239.
[9] J. Scherzer, A.J. Gruia Hydrocracking Science and Technology Marcel Dekker, New York, 1996.
[10] A. Nishijima, H. Shimada, T. Sato, Y. Yoshimura, J. Hiraishi, Polyhedron 5 (1986) 243–247.
[11] Y. Okamoto, M. Breysse, G.M. Dhar, C. Song, Catal. Today 86 (2003) 1–3.
[12] M. Breysse, J.L. Portefaix, M, Vrinat, Catal. Today 10 (1991) 489–505.
[13] G. Muralidhar, F.F. Massoth, J. Shabtai, J. Catal. 85 (1984) 44–52.
[14] J.A.R. van Veen, S.T. Sie, Technology 61 (1999) 1.
[15] W.R.A.M. Robinson, J.A.R. van Veen, V.H.J. de Beer, R.A. van Santen, Fuel Process. Technol. 61 (1999) 61.
[16] C. Leyva, S.R. Mohan, J. Ancheyta, Catal. Today 130 (2008) 345–353.
[17] R.J. Farrauto, C.H. Bartholomew, Fundamentals of Industrial Catalytic Processes, Blackie, Chapman & Hall, London, 1997, pp. 640.
[18] H. Rajesh, U.S. Ozkan, Ind. Eng. Chem. Res. 32 (1993) 1622–1630.
[19] J.J. Spivey, Ind. Eng. Chem. Res 26 (1987) 2165.
[20] S. Vigneron, P. Deprelle, J. Hermia, Catal. Today 27 (1996) 229.
[21] E.M. Cordi, P.J. O'Neill, J.L. Falconer, Appl. Catal. 14 (1997) 23–26.
[22] L.M. Gandía, M.A. Vicente, A. Gil, Appl. Catal. 38 (2002) 295–307.
[23] C. Lahousse, A. Bernier, P. Grange, B. Delmon, P. Papaefthimiou, T. Ioannides, X. Verykios, J. Catal. 178 (1998) 214–225.
[24] Z. Xu, K. Inumaru, S. Yamanaka, Appl. Catal. A 210 (2001) 217–224.
[25] M. Kang, E.D. Park, J.M. Kim, J.E. Yie, Catal. Today 111 (2006) 236–241.
[26] P.C. Liao, T.H. Fleisch, E.E. Wolf, J. Catal. 75 (1982) 396.
[27] B.E. Yoldas, Am. Ceram. Soc. Bull. 54 (1975) 289–290.
[28] J.W. Park, J.H. Jeoung, W.L. Yoou, H. Jung, H.T. Lee, D.K. Lee, Y.K. Park, Y.W. Rhee, Appl. Catal. A Gen. 274 (2004) 25–32.
[29] C.H. Wang, H.S. Weng, Appl. Catal. A Gen. 170 (1998) 73–80.
[30] D.V. Kazachkin, D.R. Luebke, V.I. Kovalchuk, J.L. d'Itri, J. SibFU 4 (2008) 303–325.
[31] A. Aristizabal, S. Contrerasa, N. Barrabes, J. Llorca, D. Tichit, F. Medina, Appl. Catal. B 110 (2011) 58–70.
[32] F. Epron, F. Gauthard, C. Piníeda, J. Barbier, J. Catal. 198 (2001) 309–318.
[33] J.R. Anderson, Structure of Metallic Catalysts, Academic Press London, 1975, pp. 478.
[34] F. Epron, F. Gauthard, J. Barbier, Appl. Catal. A Gen. 237 (2002) 253–261.
[35] Q.C. Yu, S.C. Zhang, B. Yang, Trans. Nonferrous Met. Soc. China 21 (2011) 2644–2648.
[36] E.A. Sales, T.R.O. de Souza, R.C. Santos, H.M.C. Andrade, Catal. Today 107–108 (2005) 114–119.
[37] L.E. Gómez, B.M. Sollier, M.D. Mizrahi, J.M. Ramallo López, E.E. Miró, A.V. Boix, Int. J. Hydrogen Energy 39 (2014) 3719–3729.
[38] R. Bouwman, P. Biloen, J. Catal. 48 (1977) 209.
[39] G. Corro, J.L.G. Fierro, V.C. Odilon, Catal. Commun. 4 (2003) 371–376.
[40] M. Peuckert, H.P. Bonzel, Surf. Sci. 145 (1984) 239.
[41] H.-H. Tseng, H.-Y. Lin, Y.-F. Kuo, Y.-T. Su, Chem. Eng. J. 160 (2010) 13–19.
[42] I.G. Dalla Lana, H.G. Karge, Z.M. George, J. Phys. Chem. 97 (1993) 8005–8011.
[43] H.G. Karge, I.G. Dalla Lana, J. Phys. Chem. 88 (1984) 1538–1543.
[44] G. Pacchioni, A. Clotet, J.M. Ricart, Surf. Sci. 315 (1994) 337–350.
[45] H.G. Karge, I.G. Dalla Lana, J. Phys. Chem. 88 (1984) 1538–1543.